VAMP-associated protein-A and oxysterol-binding protein–related protein 3 promote the entry of late endosomes into the nucleoplasmic reticulum

Mark F. Santos[a], Germana Rappa[a], Jana Karbanová[b], Thomas Kurth[b,c], Denis Corbeil[a,b,c,1], and Aurelio Lorico[a,d,1]

[a]Roseman Cancer Center and Department of Pathology, Roseman University College of Medicine, 10530 Discovery Drive, Las Vegas, NV, 89135, USA. [b]Biotechnology Center and Center for Molecular and Cellular Bioengineering (CMCB), Technische Universität Dresden, Tatzberg 47-49, 01307 Dresden, Germany. [c]DFG-Center for Regenerative Therapies Dresden and CMCB, Technische Universität Dresden, Fetscherstraße 105, 01307 Dresden, Germany. [d]Mediterranean Institute of Oncology Foundation, Via Penninazzo, 11, 95029 Viagrande, Italy.

Supporting Information
Supplementary Figures, Table and Videos

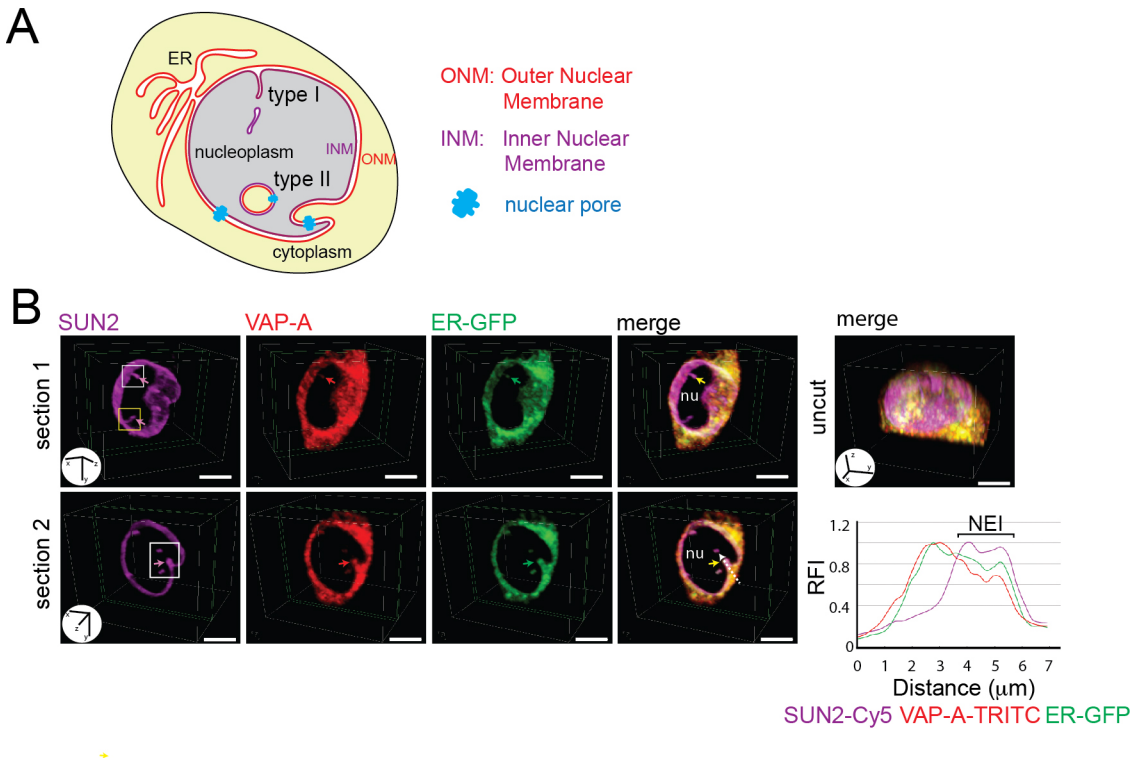

Figure S1. Types I and II NEI are found in FEMX-I cells. *A,* Schematic representation of types I and II NEI. *B,* FEMX-I cells expressing ER-GFP marker were double-immunolabeled for SUN2 and VAP-A and analyzed by CLSM. A three-dimensional (3D) reconstruction of two sections (one to three 0.4-μm-slices each) or the entire cell (uncut) are shown. The types I and II NEI are indicated with yellow and white squares, respectively. The presence of a given protein is indicated with colored arrow. The graph represents linescan analysis with relative fluorescence intensities (RFI) of each channel through the type II NEI (arrow dashed line). Note the absence of VAP-A and ER-GFP in type I NEI and the co-localization of three proteins in type II. Nu, nucleoplasm. Scale bars, 5 μm (*B*). Images depicted in section 1 (*B*) are displayed in Video S1.

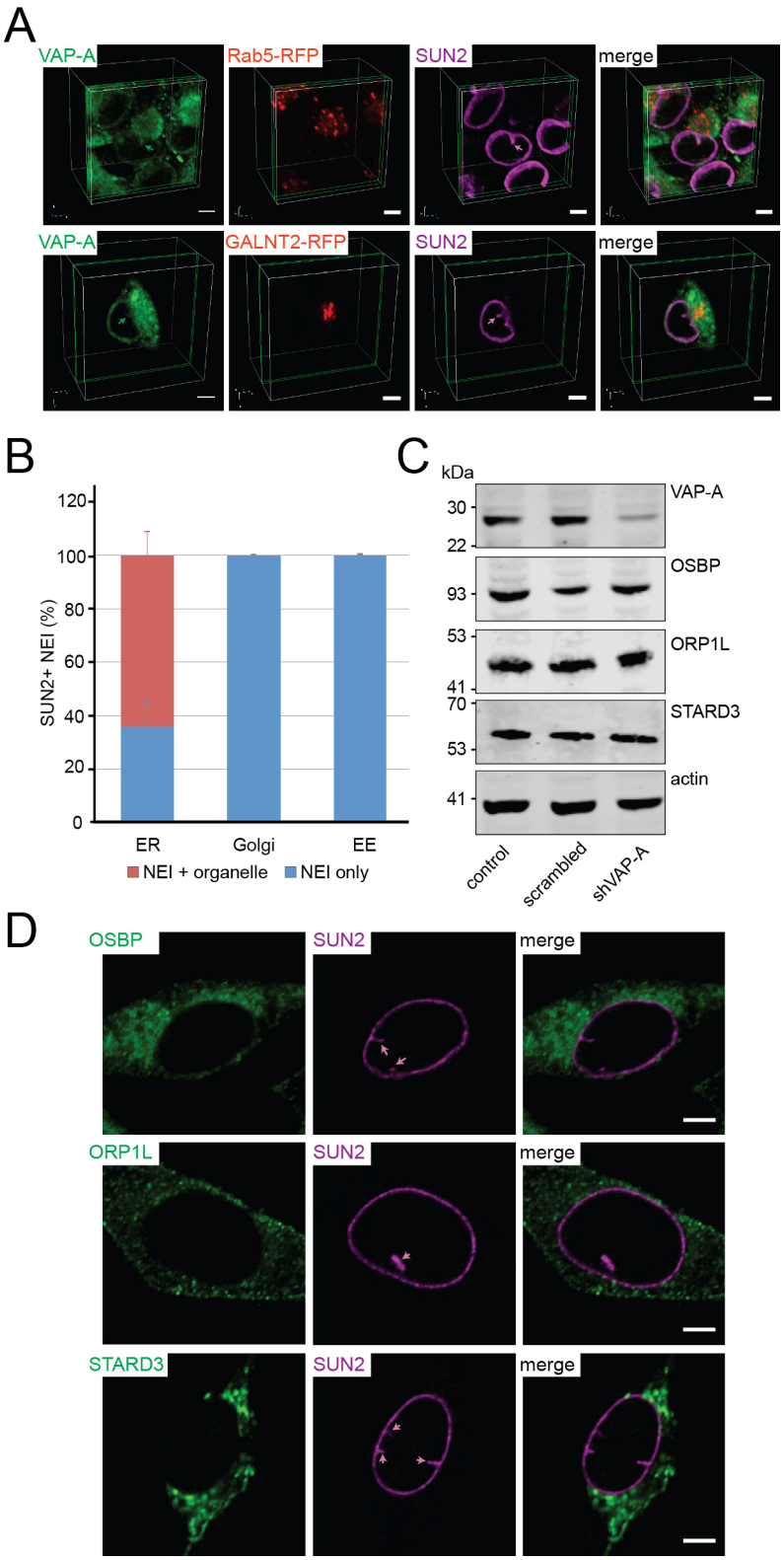

Figure S2. Early endosomes, Golgi apparatus and proteins OSBP, ORP1L and STARD3 are absent in NEI. *A, B,* FEMX-I cells expressing Rab5a- or GALNT2-RFP as markers of early endosome (EE) or Golgi apparatus (Golgi), respectively, were double-immunolabeled for VAP-A and SUN2 and analyzed by CLSM. 3D reconstruction of 2-3 adjacent sections (0.4-µm each) is presented. In each panel, arrows show the localization of a given protein in NEI. (*B*) Bar graph showing the percentage of $SUN2^{+}$ NEI

containing ER (see Figure S1B), Golgi, or EE markers. The mean ± S.D. are shown (n = 3). At least 20 cells were evaluated per experiment. *C,* Detergent lysates from untransfected (control), scrambled shRNA and shVAP-A transfected FEMX-I cells were probed for VAP-A, OSBP, ORP1L, STARD3 and β-actin by immunoblotting. Molecular mass markers (kDa) are indicated. Representative blots are shown (n = 3). *D,* FEMX-I cells were double-immunolabeled for OSBP, ORP1L or STARD3 with SUN2 and analyzed by CLSM. Note the absence of these proteins in NEI (arrows). Scale bars, 5 μm.

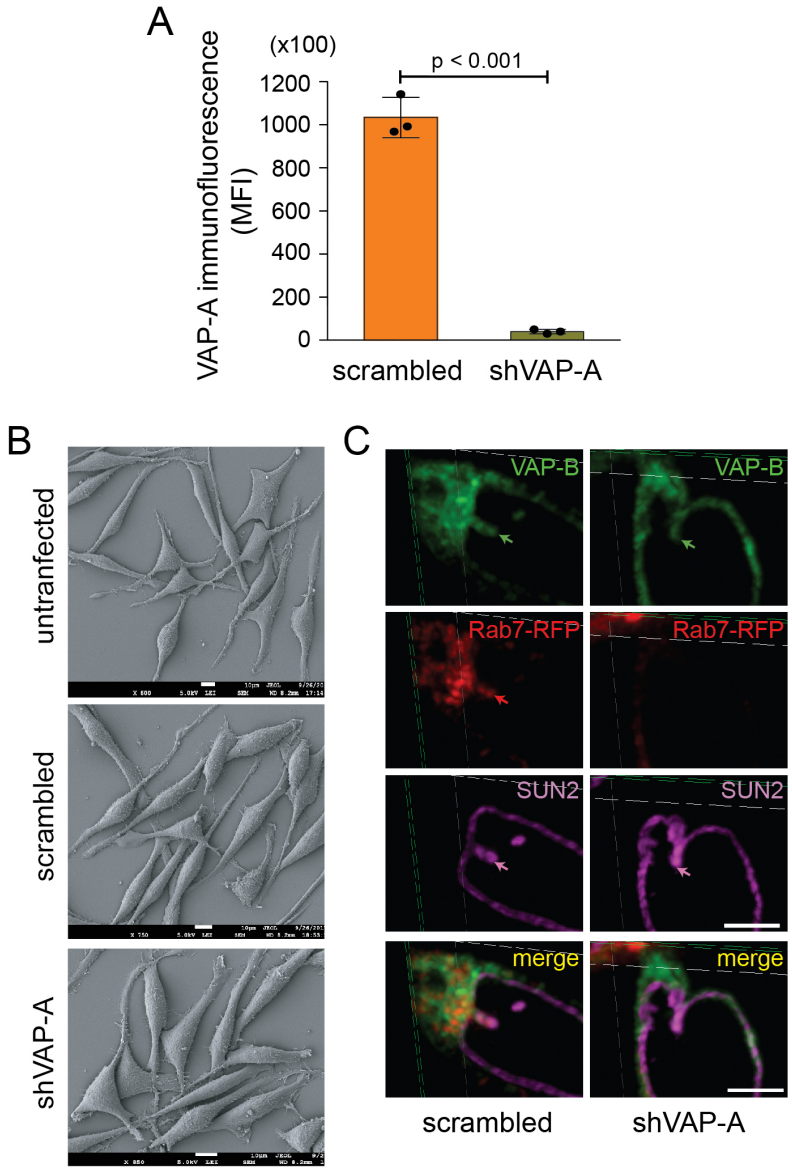

Figure S3. VAP-A silencing does not affect the localization of VAP-B in NEI. *A,* MFI of VAP-A in scrambled shRNA and shVAP-A transfected FEMX-I cells expressing Rab7-RFP. These cells were used for quantification of data presented in Figure 2*D*. The mean ± S.D. are shown (n = 3). More than 50 cells were evaluated per experiment and their average is presented. *B,* Scanning electron microscope micrographs of parental (untransfected), scrambled shRNA or shVAP-A transfected FEMX-I cells. *C,* Cells expressing Rab7-RFP were double-immunolabeled for VAP-B and SUN2 prior to CLSM. 3D reconstruction of two adjacent sections (0.4-µm each) is displayed. Arrows show the localization of a given protein in NEI. Scale bars, 10 (*B*), 5 (*C*) µm.

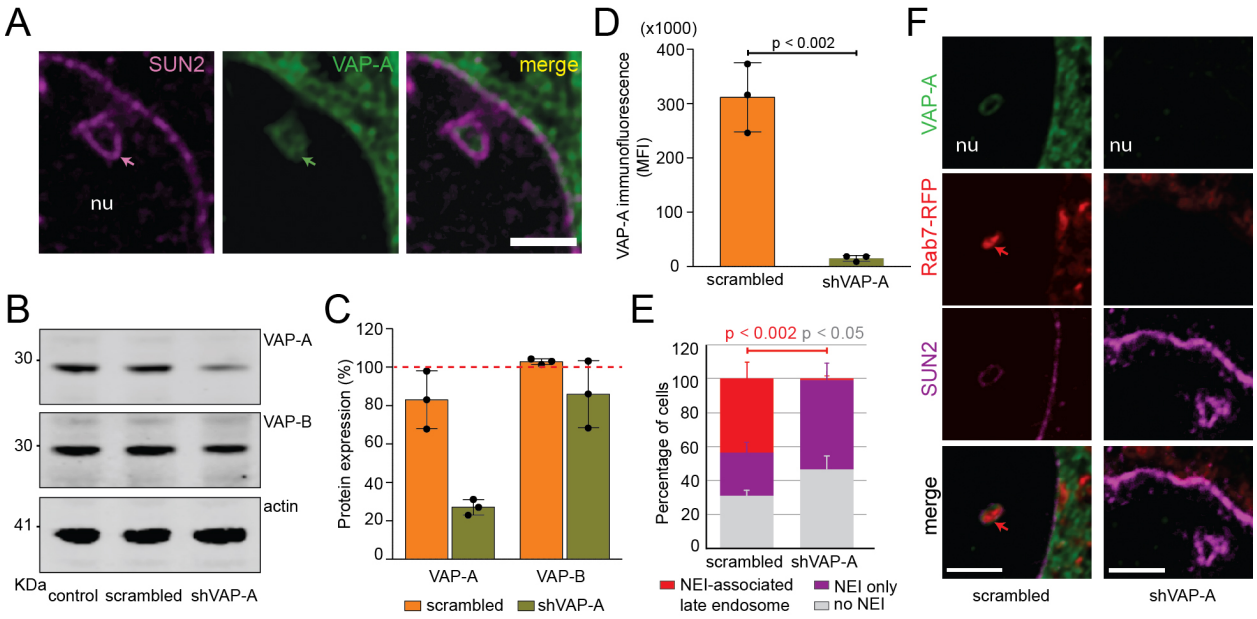

Figure S4. VAP-A is required for the entry of Rab7$^+$ late endosomes in NEI of HeLa cells. *A,* HeLa cells were double-immunolabeled for SUN2 and VAP-A and analyzed by CLSM. Arrows indicate the presence of VAP-A in SUN2$^+$ NEI. *B, C,* Detergent lysates from untransfected (control), scrambled shRNA and shVAP-A transfected HeLa cells were probed for VAP-A, VAP-B and β-actin by immunoblotting (*B*). Molecular mass markers (kDa) are indicated. Representative blots are shown. The relative expression of VAP-A or VAP-B was quantified by comparison to control samples (*C*, red dotted line). The samples were normalized using β-actin as internal loading control. The mean ± S.D. are shown with the individual value of each experience (n = 3). *D–F,* Scrambled shRNA or shVAP-A transfected cells expressing Rab7-RFP were double-immunolabeled for VAP-A and SUN2 prior to CLSM. Mean fluorescence intensity (MFI) of VAP-A in cells (*D*) used for quantification of those harboring NEI-associated Rab7$^+$ late endosomes (*E*) are presented. The mean ± S.D. are shown (n = 3). More than 50 cells were evaluated per experiment and their average is presented (*D*). Representative images showing a cross-section of NEI containing (scrambled) or not (shVAP-A) Rab7$^+$ late endosomes are presented (*F*, arrow). Nu, nucleoplasm. Scale bars, 5 µm.

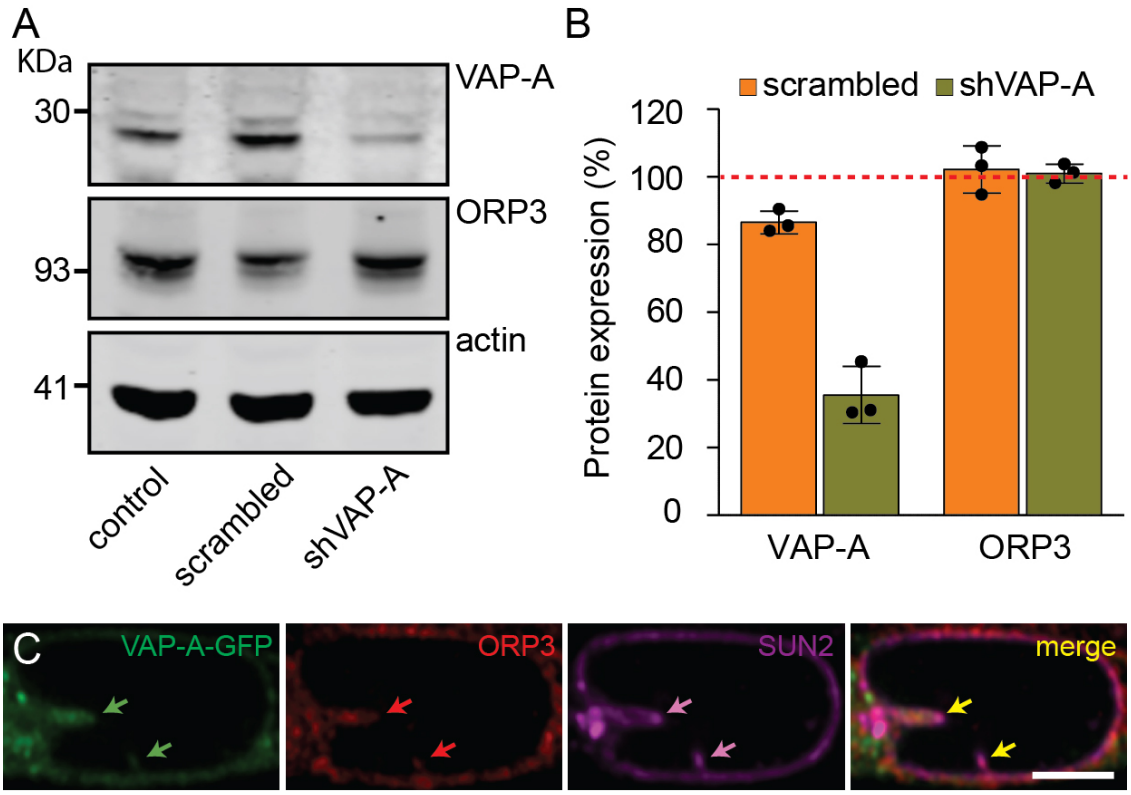

Figure S5. ORP3 expression is not affected by VAP-A silencing. *A, B,* Detergent lysates from untransfected (control), scrambled shRNA or shVAP-A transfected FEMX-I cells were probed for VAP-A, ORP3 and β-actin by immunoblotting (*A*). Molecular mass markers (kDa) are indicated. Representative blots are shown. The relative expression of VAP-A or ORP3 was quantified by comparison to control samples (*B*, red dotted line). The samples were normalized using β-actin as internal loading control. The mean ± S.D. are shown with the individual value of each experience (*B*, n = 3). *C,* FEMX-I cells expressing VAP-A-GFP were double-immunolabeled for ORP3 and SUN2 prior to CLSM. Single x-y optical section is presented. Arrows show the localization of a given protein in NEI. Scale bar, 5 µm.

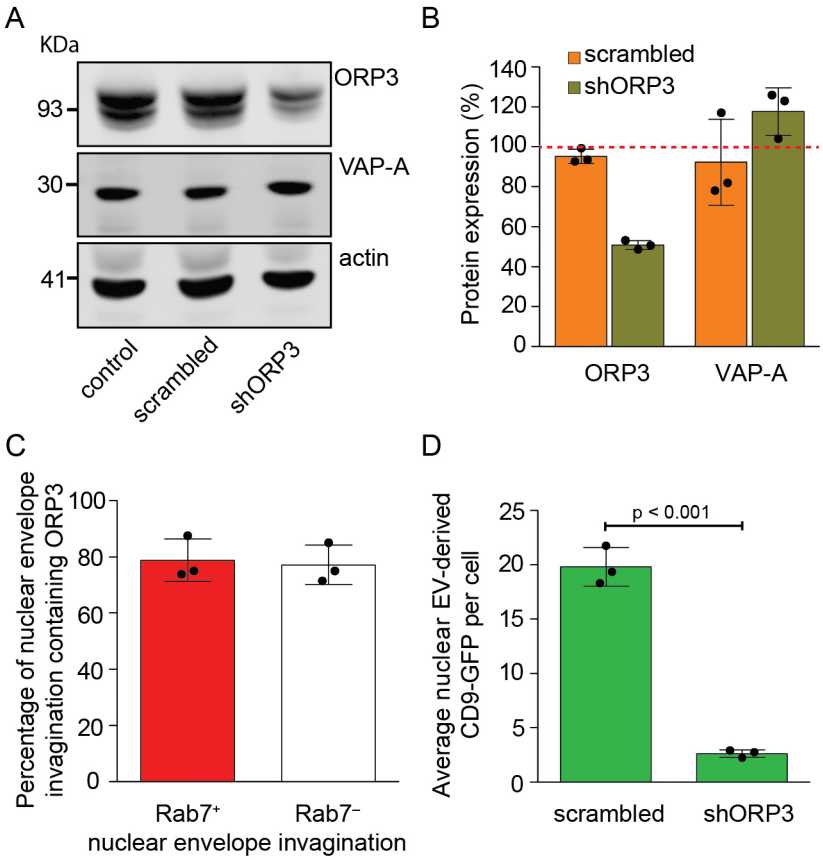

Figure S6. Expression and role of ORP3 in NEI. *A, B,* Detergent lysates from untransfected (control), scrambled shRNA and shORP3 transfected FEMX-I cells were probed for ORP3, VAP-A and β-actin by immunoblotting (*A*). Molecular mass markers (kDa) are indicated. Representative blots are shown. The relative expression of ORP3 or VAP-A was quantified by comparison to control samples (*B*, red dotted line). The samples were normalized using β-actin as internal loading control. The mean ± S.D. are shown with the individual value of each experience (n = 3). *C,* Percentage of $Rab7^+$ and $Rab7^-$ NEI containing ORP3. Cells expressing VAP-A-GFP were double-immunolabeled for ORP3 and Rab7 prior to CLSM. More than 20 $VAP\text{-}A^+$ NEI were evaluated for the presence of ORP3 and Rab7 per experiment. *D,* Scrambled shRNA or shORP3 transfected FEMX-I cells were incubated for 5 hours with 1 x 10^9 EVs derived from CD9-GFP-expressing FEMX-I cells and processed for double-immunofluorescence for ORP3 and SUN2 prior to CLSM. GFP^+ signals in the nucleoplasm were quantified using Fiji software. In both cases (*C*, *D*), mean ± S.D. are shown (n = 3). 15 NEI (*C*) or more than 30 cells (*D*) were evaluated per experiment and their averages are presented. P-value is indicated.

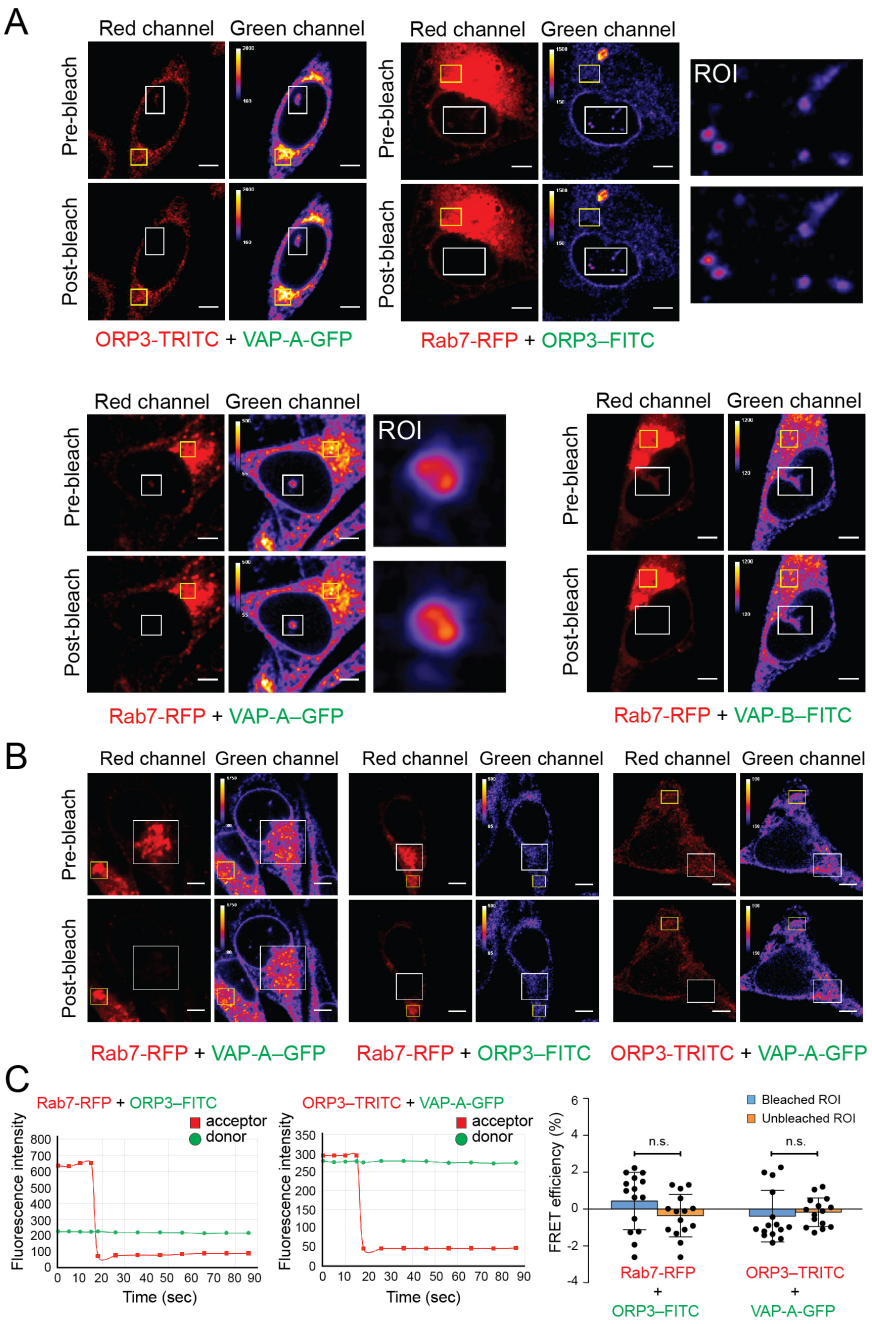

Figure S7. Interaction of ORP3 with VAP-A and Rab7 in NEI. *A, B,* Micrographs of FRET analyses of VAP-A, ORP3, and Rab7 interactions in NEI (*A*) or cytoplasm (*B*) corresponding to Figure 5. FRET pairs are indicated. An intensity profile is presented for the donor channel (GFP or FITC fluorescence). White and yellow boxes indicate bleached and unbleached areas, respectively, as ROI. The bleached ROI were magnified. *C,* FRET analysis of the interaction between ORP3 and Rab7 or VAP-A in non-NEI of nuclear membrane as ROI. FEMX-I cells expressing Rab7-RFP or VAP-A-GFP were immunolabeled for ORP3 followed by secondary antibody coupled to appropriate fluorophore (FITC or TRITC). Intensity profiles of the FRET pairs (left panels) and FRET efficiencies (right panel) are presented. The mean ± S.D. are shown (n = 3). At least 5 cells were evaluated per experiment and all of them are plotted. N.s., not significant. Scale bars, 5 µm.

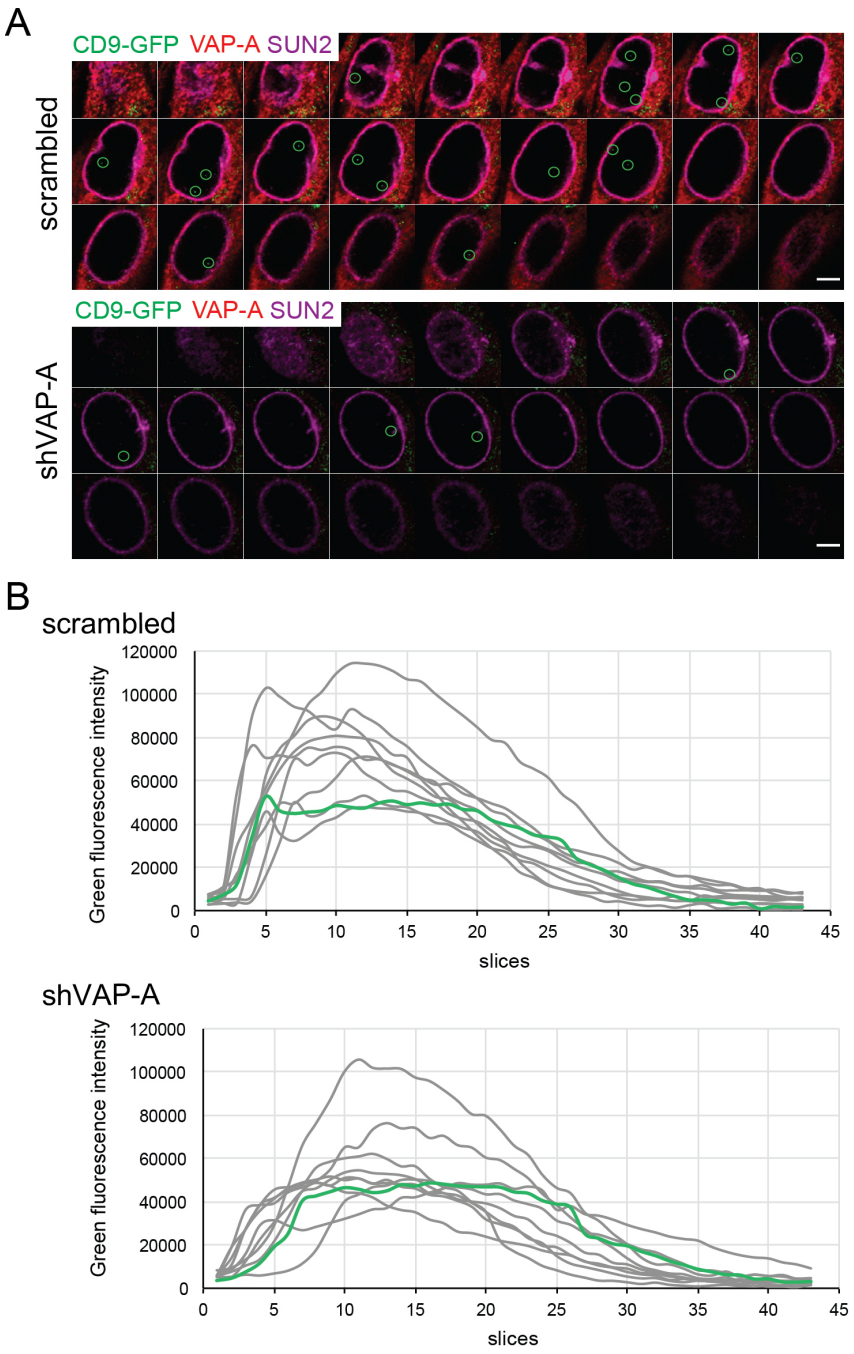

Figure S8. VAP-A is required for nuclear transfer of EV-derived proteins. *A, B,* Scrambled shRNA or shVAP-A transfected FEMX-I cells were incubated 5 hours with fluorescent EVs derived from FEMX-I cells expressing CD9-GFP and processed for double-immunofluorescence for VAP-A and SUN2 prior to CLSM. Serial x-y optical sections are presented (*A*). The discrete punctate CD9-GFP signals in the nucleoplasm are highlighted (*A*, circles) while total GFP intensity within the given cell was quantified for each slice using Fiji software (*B*). The curve of the cell displayed in panel *A* appears in green. The quantification of nuclear EV-derived CD9-GFP signals is presented in Figure 6*C* and *D*. Scale bars, 5 µm.

Supplementary Videos

Video S1. Types I and II NEI are found in FEMX-I cells.
The video depicts a FEMX-I cell expressing ER-GFP marker (green) and double-immunolabeled for VAP-A (red) and SUN2 (purple). Cell was analyzed by CLSM. 3D reconstruction with cutting plane (green slice) is displayed. Still image from this movie is shown in Fig. S1*B*. (Format: wmv; size: 19 MB).

Video S2. Presence of Rab7$^+$ late endosomes in type II NEI.
The video depicts a scrambled shRNA-transfected FEMX-I cell expressing Rab7-RFP and double-immunolabeled for VAP-A (green) and SUN2 (purple). Cell was analyzed by CLSM. 3D reconstruction with cutting plane (green slice) is displayed. Still image from this movie is shown in Fig. 2*C* (left panels). (Format: wmv; size: 19.6 MB).

Video S3. Silencing VAP-A abolishes the entry of Rab7$^+$ late endosomes in type II NEI.
The video depicts a shVAP-A-transfected FEMX-I cell expressing Rab7-RFP and double-immunolabeled for VAP-A (green) and SUN2 (purple). Cell was analyzed by CLSM. 3D reconstruction with cutting plane (green slice) is displayed. Still image from this movie is shown in Fig. 2*C* (right panels). (Format: wmv; size: 19.4 MB).

Video S4. ORP3 is found in NEI.
The video depicts a scrambled shRNA transfected FEMX-I cell expressing Rab7-RFP and double-immunolabeled for ORP3 (green) and SUN2 (purple). Cell was analyzed by CLSM. 3D reconstruction with cutting plane (green slice) is displayed. Still image from this movie is shown in Fig. 3*C* (top panels). (Format: wmv; size: 16.7 MB).

Video S5. Late endosomes containing DiI-labeled EVs enter and tether VAP-A$^+$ ONM in NEI.
The video depicts the presence of late endosomes containing DiI-labeled EVs in NEI of a FEMX-I cell expressing VAP-A-GFP. Images were acquired every 10 sec and video was made at a playing speed of 3 frames per sec. Still images from this movie are shown in Fig. 7*A* (Format: avi; size: 891 KB).

Table S1. Primary antibodies used for immunodetection.

Antigen	mAb clone / AS (host species)	Manufacturer	Dilution		
			ICC	IB	IS
SUN2	H-145 (rb)	Santa Cruz Biotechnology	1:50		
SUN2	A-10 (m)	Santa Cruz Biotechnology	1:50		
VAP-A	4C12 (m)	Novus Biologicals	1:100	1:500	
VAP-A	As (rb)	GeneTex		1:500	
VAP-A-GFP	anti-GFP (rb)	Torrey Pines	*1:100		
VAP-A-GFP	anti-GFP-conjugated to microbeads (m)	Miltenyi Biotec			1:20
VAP-B	As (rb)	Bethyl Laboratories	1:50	1:1000	1:100
ORP3	D-12 (m)	Santa Cruz Biotechnology	1:50	1:500	1:200
ORP3	As (rb)	Bethyl Laboratories	1:50	1:1000	
ORP1L	EPR8646 (rb)	Abcam	1:200	1:1000	
OSBP	As (rb)	Bethyl Laboratories	1:50	1:1000	
STARD3	As (rb)	Abcam	1:200	1:1000	
α-Tubulin	DM1A (m)	Sigma-Aldrich	1:200		
β-Actin	C4 (m)	Santa Cruz Biotechnology		1:2000	
Rab7	EPR7589-conjugated to Alexa Fluor 647 (rb)	Abcam	1:100		
Rab7	EPR7589 (rb)	Abcam	*1:10–1:50		
Rab7	As (rb)	GeneTex		1:500	
Protrudin	As (rb)	GeneTex		1:1000	

mAb, monoclonal antibody; AS, antiserum; M, mouse; Rb, rabbit
ICC, immunocytochemistry; IB, immunoblotting; IS, immunoisolation
*Immunogold labeling